

Outlining and Filling: Hierarchical Query Graph Generation for Answering Complex Questions over Knowledge Graph

Yongrui Chen, Huiying Li, Guilin Qi, Tianxing Wu, and Tenggou Wang

Abstract—Query graph building aims to build correct executable SPARQL over the knowledge graph for answering natural language questions. Although recent approaches perform well by NN-based query graph ranking, more complex questions bring three new challenges: complicated SPARQL syntax, huge search space for ranking, and noisy query graphs with local ambiguity. This paper handles these challenges. Initially, we regard common complicated SPARQL syntax as the sub-graphs comprising of vertices and edges and propose a new unified query graph grammar to adapt them. Subsequently, we propose a new two-stage approach to build query graphs. In the first stage, the top- k related instances (entities, relations, etc.) are collected by simple strategies, as the candidate instances. In the second stage, a graph generation model performs hierarchical generation. It first outlines a graph structure whose vertices and edges are empty slots, and then fills the appropriate instances into the slots, thereby completing the query graph. Our approach decomposes the unbearable search space of entire query graphs into affordable sub-spaces of operations, meanwhile, leverages the global structural information to eliminate local ambiguity. The experimental results demonstrate that our approach greatly improves state-of-the-art on the hardest KGQA benchmarks and has an excellent performance on complex questions.

Index Terms—Knowledge Graph, Question Answering, Formal Language, Query Graph

1 INTRODUCTION

As an important form of structured data, Knowledge Graph (KG) is receiving more and more attention in the field of artificial intelligence. Unlike traditional relational databases, knowledge graphs are typically stored in the form of triples, denoted as $\langle \text{subject}, \text{predicate}, \text{object} \rangle$. In order to efficiently access the KG, SPARQL, a logical formal language, is proposed as a standard interface. Unfortunately, SPARQL is not user-friendly enough because it requires an in-depth understanding on its syntax and the KG. Compared to using SPARQL, humans prefer to use Natural Language Questions (NLQ) to get the answers. Therefore, how to translate NLQ into machine-understandable SPARQL queries, is an urgent problem to be solved for Knowledge Graph Question Answering (KGQA).

There is naturally a lexical gap between SPARQL and NLQ because SPARQL aims to facilitate users to operate data but NLQ aims for daily communication. In order to build a bridge from NLQ to SPARQL, intermediate representations (e.g., λ -DCS) are proposed as a buffer. These intermediate representations are equivalent to SPARQL but hide the specific implementations (e.g., SELECT and WHERE). Query Graph [1] is a widely-used intermediate representation in recent work due to its readability. In a query graph, a topic entity, i.e., the entity mentioned in the NLQ, is connected to the answer through a core relation chain with constraints. The gray box of Fig. 1b shows an example that the query graph intuitively reflects the inference path of the NLQ. In this way, the problem of KGQA can be simplified to query graph building.

In recent research, ranking-based approaches seems to be a consensus for query graph building. Typically, these approaches consist of two stages: 1) First, the candidate query graphs are collected by a STAGG [1] strategy, which enumerates and combines all appropriate topic entities, core relation chain, and constraints in turn. 2) Then, a neural network model is employed to calculate the semantic scores between the NLQ and each candidate. The top-score candidate is finally returned. Benefiting from the powerful representation capability of neural networks, these approaches achieve good performance.

Challenge However, more and more complex NLQs bring three new challenges for existing approaches: *Complicated SPARQL Syntax* (challenge 1) The SPARQL corresponding to complex NLQs often comprise complicated syntax of ORDER BY, FILTER, aggregation functions (e.g., MAX and COUNT) and even nested queries. Fig 1a shows an SPARQL query S_0 (green dotted box) that contains a sub-query S_1 (golden dotted box). It can not be represented by a simple constraint nodes attaching to the core relation chain so that troubles the conventional query graph. *Huge Search Space* (challenge 2) Because of the enumeration of STAGG, the size of the candidate query graph set can be approximately $|\mathcal{V}| \approx Y^L$, where L is the maximum length of the core relation chain and Y is the average number of one-hop candidate relations. For a complex NLQ, L often exceeds 3 (dotted path in \mathcal{G}_1 of Fig. 1b), and Y ranges from tens to hundreds. Consequently, the resulting \mathcal{V} is typically ranges thousands to millions. Such a huge quantity makes the embedding of neural networks impractical due to the space limitation of hardware. *Local Ambiguity* (challenge 3) The enumeration also produces some confusing query graphs. These graphs is wrong in terms of global semantic information while have

• Y. Chen, H. Li, G. Qi, T. Wu, and T. Wang are with School of Computer Science and Engineering, Southeast University, Nanjing 210096, China. E-mail: {yrcen, huiyingli, gqi, tianxingwu, wangtenggou}@seu.edu.cn

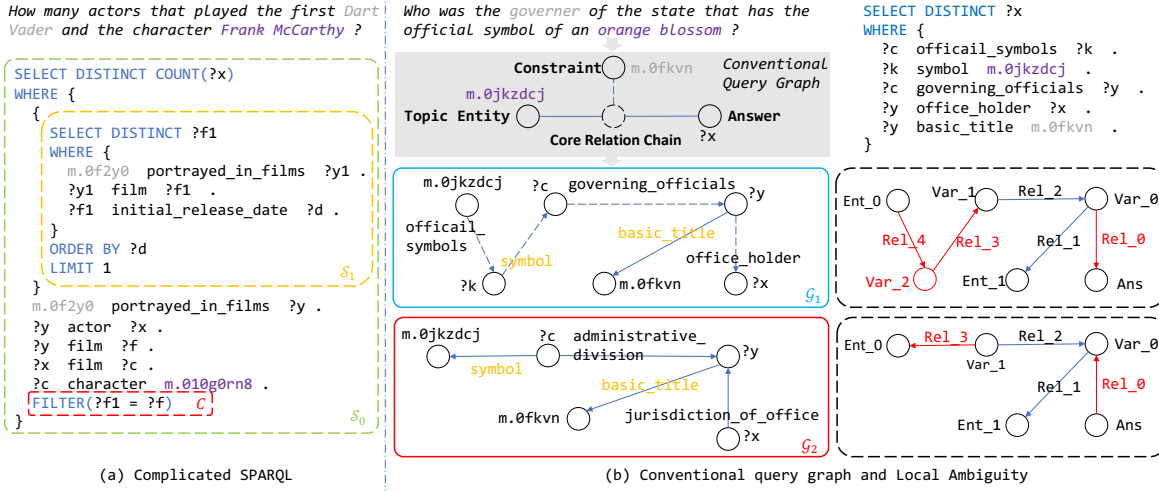


Fig. 1: Examples of challenges. (a) shows a complicated SPARQL program in ComplexWebQuestions [2], which has a nested query. (b) shows an example of the local ambiguity. The blue and red boxes are the correct and the wrong query graph, respectively, and the dotted boxes are their structures. Here, we only use the short name of each relation for clarity.

some components locally correct. For example, in Fig. 1b, G_1 (blue box) is the correct query graph and G_2 (red box) is a confusing one while has the correct entities $m.0jkzdcj$ and $m.0fkvn$, and correct relations `symbol` and `basic_title`. The model suffers from these local ambiguous components thence making wrong prediction.

Motivation In this paper, we focus on how to address the three challenges. For challenge 1, we observe that no matter how complex the SPARQL syntax is, it can be broken into entities, variables, values, relations, and other built-in properties. If regarding these fine-grained components as vertices and edges, the resulting query graph should have a stronger representation capability. For challenge 2, some related work [3], [4], [5] reveals that generation can decompose the large total search space into much smaller sub-spaces. If the query graph is generated by multiple steps, the model only needs to embed the candidate decisions at each step, thus avoid the unaffordable cost of space for representing all the candidate query graphs. For challenge 3, we observe that structure of the query graph is efficient on disambiguation. The two dotted boxes in Fig. 1b outline the structures of G_1 and G_2 , respectively. Compared with G_1 , G_2 has one less variable node Var_2 , and the wrong directions of relations Rel_0 and Rel_3 . Therefore, if the structure is correctly predicted, the local ambiguity can be greatly reduced (challenge 3). Furthermore, structure prediction should be easier to instance prediction since the diversity of the former is usually far lower than that of the latter.

Our Approach Based on the motivation above, we propose a new approach for query graph building. First, we redefine a query graph that treats `ORDER BY`, `FILTER`, aggregation functions, and nested queries as the sub-graphs composed of vertices and edges. Subsequently, to describe the structure of redefined query graphs, we propose an Abstract Query Graph (AQG). It retains the topology of the query graph while its vertices and edges are slots of categories without instances. Finally, we propose a *Hierarchical Graph Generation Network* (HGNet) to generate query graphs. Specifically, our

propose approach consists of two stages. In the first stage, for each category (e.g., entity, relation, and value), the top- k related instances are collected by a simple strategy (e.g., relation ranking and pattern matching), as the candidate pool. In our running example in Fig. 1a, “1” is a candidate value. In the second stage, HGNet first encodes the NLQ and then performs autoregressive decoding to generate the query graph from scratch. Specifically, the decoding procedure is hierarchical that comprises two phases, namely *Outlining* and *Filling*. *Outlining* begins with an empty graph and targets generating an AQG. At each step, the model expands the graph by predicting and adding a slot vertex or slot edge to the graph. When receiving a self-ending signal, the AQG is completed. *Filling* begins with the AQG and targets generating a query graph. At each step, the model predicts an instance from the candidate pool and fills it to the corresponding slot vertex or slot edge. When all the slots are filled, the query graph is finally obtained. Because *Outlining* focuses on structures, HGNet employs a graph encoding module to capture the entire structural information of the current graph at each decoding step during *Outlining*. We conduct comprehensive experiments on existing KGQA benchmarks. HGNet outperforms all the existing approaches on both ComplexWebQuestions [2] and LC-QuAD [6], and a competitive result on WebQSP [7]. Especially on the ComplexWebQuestions, the currently most complex KGQA benchmark, HGNet substantially improves state-of-the-art by 20.9% in terms of F1-score.

2 PRELIMINARIES

2.1 Knowledge Graph

A knowledge graph (KG) is typically a collection of subject-predicate-object triples, denoted by $\mathcal{K} = \{\langle s, p, o \rangle \mid s \in \mathcal{E}, p \in \mathcal{R}, o \in \mathcal{E} \cup \mathcal{L}\}$, where \mathcal{E} , \mathcal{R} and \mathcal{L} denote the entity set, relation set, and literal set, respectively. If o is an entity, $\langle s, p, o \rangle$ denotes that relation p exists between head entity s and tail entity o . If o is a literal, $\langle s, p, o \rangle$ denotes that the entity s has a property p , value of which is o .

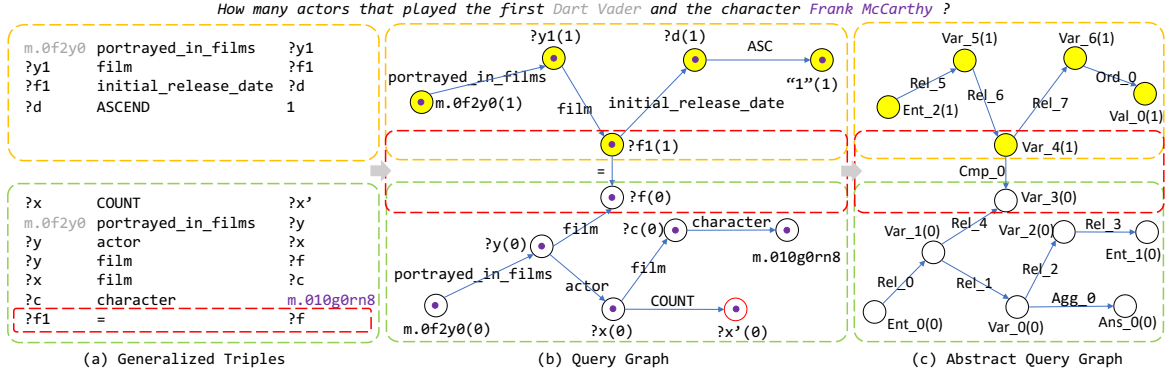


Fig. 2: An example of generalized triples, query graphs, and abstract query graphs. The dotted boxes of the same color mean the corresponding relationship, including Fig. 1a. In (b) and (c), the number in the parenthesis after each vertex name is its segment number. The red circle, i.e., $?x'(0)$ in (b), is the vertex that represents the answer.

2.2 Query Graph

In order to adapt complicated SPARQL syntax, we redefine the query graph as follows.

Definition 1 (Query Graph). A query graph is a directed acyclic graph, denoted by $\mathcal{G}_q = (V_q, E_q, \Psi_q, \Phi_q, S_q)$. Here, V_q is the vertex set and $E_q = \{e | e = \langle v, v' \rangle, v, v' \in V_q\}$ is the edge set. $\Psi_q = \{(v, l_v) | v \in V_q\}$, where $l_v \in \Psi$ is a vertex label and Ψ denotes the set of entities, types, values, and variables. $\Phi_q = \{(e, l_e) | e \in E_q\}$, where $l_e \in \Phi$ is an edge label and Φ denotes the set of relations and built-in properties. $S_q = \{(v, s_v) | v \in V_q\}$, where s_v denotes the segment number of v .

The redefined query graph is able to represent `FILTER`, `ORDER BY`, aggregation functions, and nested queries. Fig. 2a illustrates how to convert the complicated SPARQL in our running example to a query graph. First, the SPARQL query is parsed to generalized triples, of which the predicate can be either a KG relation or built-in property. In the example, the generalized triples consist of relation triples (e.g., $\langle ?y1, \text{film}, ?f1 \rangle$), comparison triples (e.g., $\langle ?f1, =, ?f \rangle$), order triples (e.g., $\langle ?d, \text{ASCEND}, 1 \rangle$), and aggregation triples (e.g., $\langle ?x, \text{COUNT}, ?x' \rangle$). The total generalized triples are extracted from the main query (green box) and each sub-query (golden box) and then merged. For each triple, the subject and object are regarded as vertices, and the predicate as an edge, then the query graph (Fig. 2b) is obtained. For more complicated cases, such as temporal intervals and sub-queries with `?x` intention, Appendix A details the solutions. The obtained query graph has the following two properties.

Property 1. $\forall v_1, \forall v_2 \in V_q$, if $s_{v_1} = s_{v_2}$, then v_1 and v_2 are from the same segment of the SPARQL.

where the segment is a sub-query or the main query of the SPARQL. In our query graph, the segment number of the main query is always set to 0, such as green box in Fig. 2b.

Property 2. $\forall \mathcal{G}_q = (V_q, E_q, \Psi_q, \Phi_q, S_q)$, $|V_q| = |E_q| + 1$.

Obviously, a segment is weakly connected and any meaningful sub-segment ($s_v > 0$) is associated with the main segment ($s_v = 0$) through the `FILTER` clause (red box). Therefore, a query graph is always weakly connected, i.e. $|V_q| \leq |E_q| + 1$. In this paper, we further simplify the

problem by only focusing on the query graphs that satisfy $|V_q| = |E_q| + 1$. Although the assumption is strengthened, in the hardest ComplexWebQuestions [2] dataset, there are still 98.5% of SPARQL queries meet it.

In our query graph, `FILTER`, `ORDER BY`, aggregation functions, and nested queries are all induced into a unified graph grammar, which is promising to be generated by a grammar-based autoregressive manner. In the rest of this paper, each query graph refers to our redefined one.

2.3 Abstract Query Graph

The structure of a query graph is reflected in the categories and topology of its vertices and edges thence we propose an Abstract Query Graph (AQG) as follows.

Definition 2 (Abstract Query Graph). An abstract query graph is a directed acyclic graph, denoted by $\mathcal{G}_a = (V_a, E_a, \Psi_a, \Phi_a, S_a)$. Here, V_a is the set of vertices and $E_a = \{e | e = \langle v, v' \rangle, v, v' \in V_a\}$ is set of edges. $\Psi_a = \{(v, c_v) | v \in V_a\}$, where $c_v \in \Psi$ is a vertex class and $\Psi = \{\text{Ans}, \text{Var}, \text{Ent}, \text{Type}, \text{Val}\}$. $\Phi_a = \{(e, c_e) | e \in E_q\}$, where $c_e \in \Phi$ is an edge class and $\Phi = \{\text{Rel}, \text{Ord}, \text{Cmp}, \text{Agg}\}$. $S_a = \{(v, s_v) | v \in V_a\}$, where s_v denotes the segment number of v .

where Φ and Ψ are the class label sets of vertices and edges, respectively. The meaning of each label is as follows.

`Ans` denotes the only one answer in the query graph, such as `?x` in Fig. 2b. `Var` denotes the variables, which are placeholders for unknown vertices except the answer, such as all vertices prefixed with `?`. `Ent` denotes entities, such as `m.0f2y0`. `Type` denotes the types that describe a set of entities, such as `Actor` (in *DBpedia*) and `award.award_winner` (in *Freebase*). `Val` denotes the values, such as `"1"` and `"2011-01-01"`. `Rel` denotes KG relations, such as `portrayed_in_films`. `Ord` denotes `{ASC, DESC}` in `ORDER BY` clauses. For example, triple $\langle ?v \text{ ASC } 3 \rangle$ means `ORDER BY ASC(?v) LIMIT 3`. `Cmp` denotes `{=, \neq, >, \geq, <, \leq, \text{DURING}, \text{OVERLAP}}` that describes the comparison relationships between variables and values. Here `DURING` and `OVERLAP` are used to handle temporal intervals, detailed in Appendix A.1. `Agg` denotes `{COUNT, MAX, MIN, ASK}` that describe the aggregation functions on the variables or answers. For example, triple

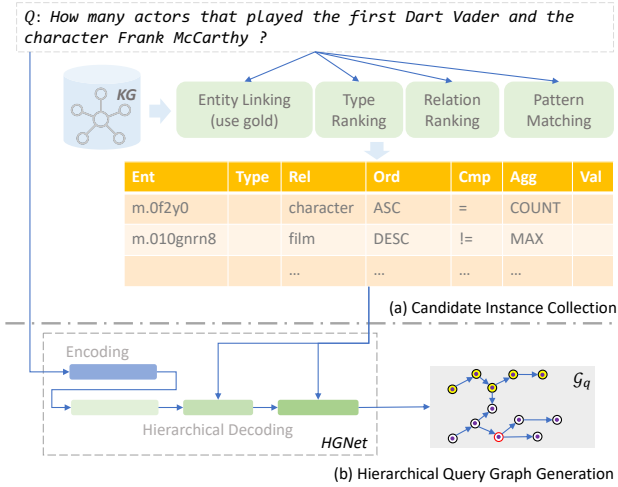


Fig. 3: Entire process of our proposed approach.

$\langle ?x \text{ COUNT } ?y \rangle$ means that $?y$ is the count number of variable $?x$.

Fig. 2c exhibits the AQG of the running example. The AQG inherits the structure of the query graph, thereby naturally has the following two properties.

Property 3. $\forall v_1, \forall v_2 \in V_a, (v_1, s_{v_1}), (v_2, s_{v_2}) \in S_a$, if $s_{v_1} = s_{v_2}$, then v_1 and v_2 correspond to the same segment.

Property 4. $\forall \mathcal{G}_a = (V_a, E_a, \Psi_a, \Phi_a, S_a)$, $|V_a| = |E_a| + 1$.

Each vertex and edge of the AQG can be regarded as a slot of the abstract class. A query graph \mathcal{G}_q can be converted to a unique AQG \mathcal{G}_a by replacing the instances with the corresponding class slots, on the contrary, an AQG \mathcal{G}_a can also generate a series of query graphs $\{\mathcal{G}_q^i\}$ by filling all the class slots with a combination of instances. Formally, let $\mathcal{F} : \mathbf{G}_Q \rightarrow \mathbf{G}_A$ as a n -to-one mapping, where \mathbf{G}_Q and \mathbf{G}_A are respectively the domains of query graphs and AQGs, $\mathcal{F}^{-1} : \mathbf{G}_A \rightarrow \mathbf{G}_Q$ as the inverse one-to- n mapping of \mathcal{F} , then there are the following two properties.

Property 5. $\forall \mathcal{G}_q^1, \forall \mathcal{G}_q^2 \in \mathbf{G}_Q$ is structurally equivalent, if and only if $\mathcal{F}(\mathcal{G}_q^1) = \mathcal{F}(\mathcal{G}_q^2)$.

Property 6. $\forall \mathcal{G}_a^1, \forall \mathcal{G}_a^2 \in \mathbf{G}_A$, if $\mathcal{G}_a^1 \neq \mathcal{G}_a^2$, then $\mathcal{F}^{-1}(\mathcal{G}_a^1) \cap \mathcal{F}^{-1}(\mathcal{G}_a^2) = \emptyset$.

Property 6 reveals that two resulting query graph sets from different AQGs are disjoint. Therefore, if the AQG \mathcal{G}_a is determined first, the search space of \mathcal{G}_q can significantly reduced from the full domain \mathbf{G}_Q to \mathbf{G}'_Q , where $\mathbf{G}'_Q = \mathcal{F}^{-1}(\mathcal{G}_a)$ and $|\mathbf{G}'_Q| \ll |\mathbf{G}_Q|$.

3 OVERVIEW

Fig. 3 illustrates the process overview of our proposed approach, which consists of the following two stages.

3.1 Candidate Instance Collection

As mentioned in Section 2.3, the classes of instances can be generalized as $\Psi \cup \Phi = \{\text{Ans}, \text{Var}, \text{Ent}, \text{Rel}, \text{Type}, \text{Val}, \text{Ord}, \text{Cmp}, \text{Agg}\}$. Excluding classes Ans and Var that have no instances, the instances of the remaining classes

are collected by the strategies including type linking, relation linking, and pattern matching. Each strategy will be detailed in Section 4. The obtained instances are regarded as the candidate components, denoted by $\mathcal{I} = \{\mathcal{I}_x | x \in \Psi \cup \Phi - \{\text{Ans}, \text{Var}\}\}$, where \mathcal{I}_x denotes the candidate instance set of class x .

3.2 Hierarchical Query Graph Generation

Based on \mathcal{I} , our HGNet first encodes Q and then generates a query graph \mathcal{G}_q by autoregressive decoding of two levels.

At the high-level decoding process, HGNet starts from an empty graph and expands it to an AQG \mathcal{G}_a by a sequence of the graph-based operations. Specifically, at each step, the model first predicts an operation with the combined information of the question and previous graph and then executes it to obtain a new graph. We call this process *Outlining*, detailed in 5.1.

At the ground-level decoding process, HGNet begins with \mathcal{G}_a and instantiates it to a query graph \mathcal{G}_q by a sequence of operations. Concretely, at each step, the model focuses on a slot in \mathcal{G}_a , denoted by x , and predicts an instance $i \in \mathcal{I}_{c_x}$ to fill x . We call this process *Filling*, which is detailed in 5.2. When all the slots (except Var and Ans) in \mathcal{G}_a are filled with the instances, final query graph \mathcal{G}_q is completed.

4 CANDIDATE INSTANCE COLLECTION

For class Ord, Cmp, and Agg, the candidate instances are obtained by the enumeration. Specifically, $\mathcal{I}_{ord} = \{\text{ASC}, \text{DESC}\}$, $\mathcal{I}_{cmp} = \{=, \neq, >, \geq, <, \leq, \text{DURING}, \text{OVERLAP}\}$, and $\mathcal{I}_{agg} = \{\text{COUNT}, \text{MAX}, \text{MIN}, \text{ASK}\}$. These built-in properties are so few that not necessary to screen. For class Val, candidate instance set \mathcal{I}_{val} is extracted from Q by pattern matching. We summarize the types of values: integers, floating numbers, quoted strings, year, and date. Because these values are often based on specific patterns, we designed regular expressions to extract them. For class Rel, \mathcal{I}_{rel} is obtained by relation ranking [8]. Concretely, we train a naive BiLSTM as the ranker to encode Q and each one-hop relation $r \in \mathcal{R}$ and calculate their semantic relevance score. The top- k relations with highest score are returned. The ranker is trained by optimizing the hinge loss of positive and negative relations. Here, the positive relations are obtained from the gold SPARQL and the negative are randomly sample from \mathcal{R} . For class Type, \mathcal{I}_{type} is obtained by a similar approach with Rel. The only difference is that we add a type NONE here to indicate the case that there is no type in Q . If the top-1 type is NONE, there is no candidate instance returned. For class Ent, in order to make a fair comparison with previous work [9], [10], [11], [12], we follow them that directly extract the gold entities from the gold SPARQL as the candidate instances. In our running example, $\mathcal{I}_{ent} = \{m.0f2y0, m.010gnrn8\}$.

It needs to emphasized that, the goal of the strategies above are only for high-quality candidate instance sets and it is allowed to use any alternative manners.

5 HIERARCHICAL GENERATION FRAMEWORK

5.1 Outlining Process

The goal of *Outlining* is to generate an AQG with \mathcal{N} vertices and $\mathcal{N} - 1$ edges, where \mathcal{N} is unknown. The process can be

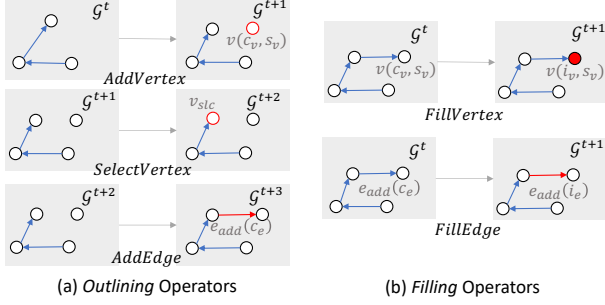


Fig. 4: Operators in our hierarchical generation framework. The red objects represent the concerned vertices and edges.

described by a sequence of graphs, $\{\mathcal{G}^0, \mathcal{G}^1, \dots, \mathcal{G}^T\}$, where $T = 3N - 1$ and $\mathcal{G}^t = (V^t, E^t, \Psi^t, \Phi^t, S^t)$ is the graph generated at step t ($0 \leq t \leq T$). In particular, $\mathcal{G}^0 = (\emptyset, \emptyset, \emptyset, \emptyset, \emptyset)$ is an empty graph and \mathcal{G}^T is the completed AQG, i.e., \mathcal{G}_a . For $t \geq 1$, the graph at step t is obtained by performing an outlining operation on the graph at step $t - 1$, i.e., $\mathcal{G}^t = f^t(\mathcal{G}^{t-1}, *a^t)$. Here, f^t denotes the Outlining operator to expand the graph at time step t and $*a^t$ denotes the arguments of f^t . According to the characteristics of the AQG, we define the following three Outlining operators, which are shown in Fig. 4a.

(a) *AddVertex* For graph $\mathcal{G}^t = (V^t, E^t, \Psi^t, \Phi^t, S^t)$, operation $AddVertex(\mathcal{G}^t, c_v, s_v, v)$ represents that a new vertex v is added into \mathcal{G}^t to return a new graph, denoted by $\mathcal{G}^{t+1} = (V^t \cup \{v\}, E^t, \Psi^t \cup \{(v, c_v)\}, \Phi^t, S^t \cup \{(v, s_v)\})$. $c_v \in \Psi \cup \{\text{End}\}$ denotes the class label of v ; s_v denotes the segment number of v . Note that End is an additional class denotes the signal of ending. If $c_v = \text{End}$, no new vertex is added to \mathcal{G}^t and Outlining is terminated.

(b) *SelectVertex* For graph $\mathcal{G}^{t+1} = (V^t \cup \{v\}, E^t, \Psi^t \cup \{(v, c_v)\}, \Phi^t, S^t \cup \{(v, s_v)\})$, operation $SelectVertex(\mathcal{G}^{t+1}, u, v)$ represents that vertex $u \in V^t$ is selected, to connect to vertex v in the next step. Note that there is no difference in structure between \mathcal{G}^{t+1} and the returned new graph. However, to explicitly show this operation, the new graph is denoted by \mathcal{G}^{t+2} .

(c) *AddEdge* For graph $\mathcal{G}^{t+2} = (V^t \cup \{v\}, E^t, \Psi^t \cup \{(v, c_v)\}, \Phi^t, S^t \cup \{(v, s_v)\})$, $AddEdge(\mathcal{G}^{t+2}, c_e, e)$ represents that a new edge $e = \langle u, v \rangle$ (or $\langle u, v \rangle$) is added into \mathcal{G}^{t+2} . The new graph is denoted by $\mathcal{G}^{t+3} = (V^t \cup \{v\}, E^t \cup \{e\}, \Psi^t \cup \{(v, c_v)\}, \Phi^t \cup \{(e, c_e)\}, S^t \cup \{(v, s_v)\})$, where $c_e \in \Phi$ is the class label of e . Note that c_e has a direction $+$ or $-$, e.g., $Rel+$ means the relation is from u to v , $Rel-$ means v to u .

As shown in Fig. 4a, successively performing *AddVertex*, *SelectVertex*, and *AddEdge* can add a new edge $\langle u, v \rangle$ into the graph. In Outlining, f^t is pre-determined for each step t . Concretely, the first operation is specified as *AddVertex*, which converts the initial empty graph $\mathcal{G}^0 = (\emptyset, \emptyset, \emptyset, \emptyset, \emptyset)$ into $\mathcal{G}^1 = (\{v_0\}, \emptyset, \{(v, c_v)\}, \emptyset, \{0\})$. Then, the AQG is gradually generated by performing *AddVertex*, *SelectVertex*, and *AddEdge* in loop. The final operation is always *AddVertex* that selects End to break the loop. Formally, for $t \geq 1$,

$$f^t = \begin{cases} AddVertex & t = 1 \text{ or } t \bmod 3 = 2 \\ SelectVertex & t \bmod 3 = 0 \\ AddEdge & t > 1 \text{ and } t \bmod 3 = 1 \end{cases} \quad (1)$$

Although all the operators are fixed, different arguments $*a^t$ result in different AQG. For example, different u of *Select Vertex* makes the connections of different vertex pairs, thereby producing different topologies. It demonstrates the diversity of the query graphs generated by Outlining.

Notably, for *AddVertex*, argument v is only an id of the added vertex; for *SelectVertex*, argument v is consistent with the previous *AddVertex*; for *AddEdge*, u and v are consistent with previous *AddVertex* and *SelectVertex*, respectively. Consequently, at each time step, only c_v and s_v of *AddVertex*, u of *SelectVertex*, and c_e of *AddEdge*, need to be determined.

5.2 Filling Process

The goal of *Filling* is to convert the AQG obtained by Outlining into a query graph, whose vertices and edges are all instances rather than class labels. Similar to Outlining, *Filling* also can be described by a sequence of graphs, $\{\mathcal{G}^0, \mathcal{G}^1, \dots, \mathcal{G}^{T'}\}$, where $T' = 2N - 1$ and $\mathcal{G}^t = (V^t, E^t, \Psi^t, \Phi^t, S^t)$ is the graph generated at time step t ($0 \leq t \leq T'$). In particular, $\mathcal{G}^0 = \mathcal{G}_a$ and $\mathcal{G}^{T'}$ is the completed query graph \mathcal{G}_q . At each step $t \geq 1$, $\mathcal{G}^t = g^t(\mathcal{G}^{t-1}, *b^t)$, where g^t denotes the Filling operator to instantiate a vertex/edge and $*b^t$ denotes the arguments. We define the following two Filling operators shown in Fig. 4b.

(a) *FillVertex* For graph $\mathcal{G}^t = (V^t, E^t, \Psi^t, \Phi^t, S^t)$, operation $FillVertex(\mathcal{G}^t, v, i_v)$ represents that vertex v in \mathcal{G}^t is filled with i_v to return a new graph, i.e., $\mathcal{G}^{t+1} = (V^t, E^t, \Psi^t - \{(v, c_v)\} \cup \{(v, i_v)\}, \Phi^t, S^t)$. The first argument $v \in V^t$ denotes the vertex to be instantiated and c_v is the class label of v ; The second $i_v \in \mathcal{I}_{c_v}$ denotes an instance of class c_v .

(b) *FillEdge* For graph $\mathcal{G}^t = (V^t, E^t, \Psi^t, \Phi^t, S^t)$, operation $FillEdge(\mathcal{G}^t, e, i_e)$ represents that edge e in \mathcal{G}^t is filled with i_e to return a new graph, i.e., $\mathcal{G}^{t+1} = (V^t, E^t, \Psi^t, \Phi^t - \{(e, c_e)\} \cup \{(e, i_e)\}, S^t)$. The first argument $e \in E^t$ denotes the edge to be instantiated and c_e is the class label of e ; The second argument $i_e \in \mathcal{I}_{c_e}$ denotes an instance of class c_e .

Different from vertices, edges (e.g., relations) are so not explicit that more difficult to recognize. Therefore, we first perform vertex Filling and then edge Filling to reduce error propagation. Formally, assume that the generated \mathcal{G}_a has N vertices and $N - 1$ edges, for $t \geq 1$, g^t is determined by

$$g^t = \begin{cases} FillVertex & t \leq N \\ FillEdge & N < t \leq 2N - 1 \end{cases} \quad (2)$$

The first argument of each Filling operation is fixed by Outlining. Specifically, at step t of Filling, argument v of *FillVertex* denotes the vertex added by *AddVertex* in step $t' = 3t - 4$ of Outlining; argument e of *FillEdge* denotes the edge added by *AddEdge* in step $t' = 3t - 2 + N$ of Outlining. As a result, in order to complete Filling, only i_v of *FillVertex* and i_e of *FillEdge* need to be predicted.

6 HIERARCHICAL GRAPH GENERATION MODEL

Fig. 5 shows the architecture of our proposed HGNet, used to predict the arguments above. As Outlining focuses on structural information while Filling on instance information, we employ three decoders for Outlining, vertex Filling, and edge Filling, respectively. Moreover, to make the model completely aware of the structure of the entire graph at each

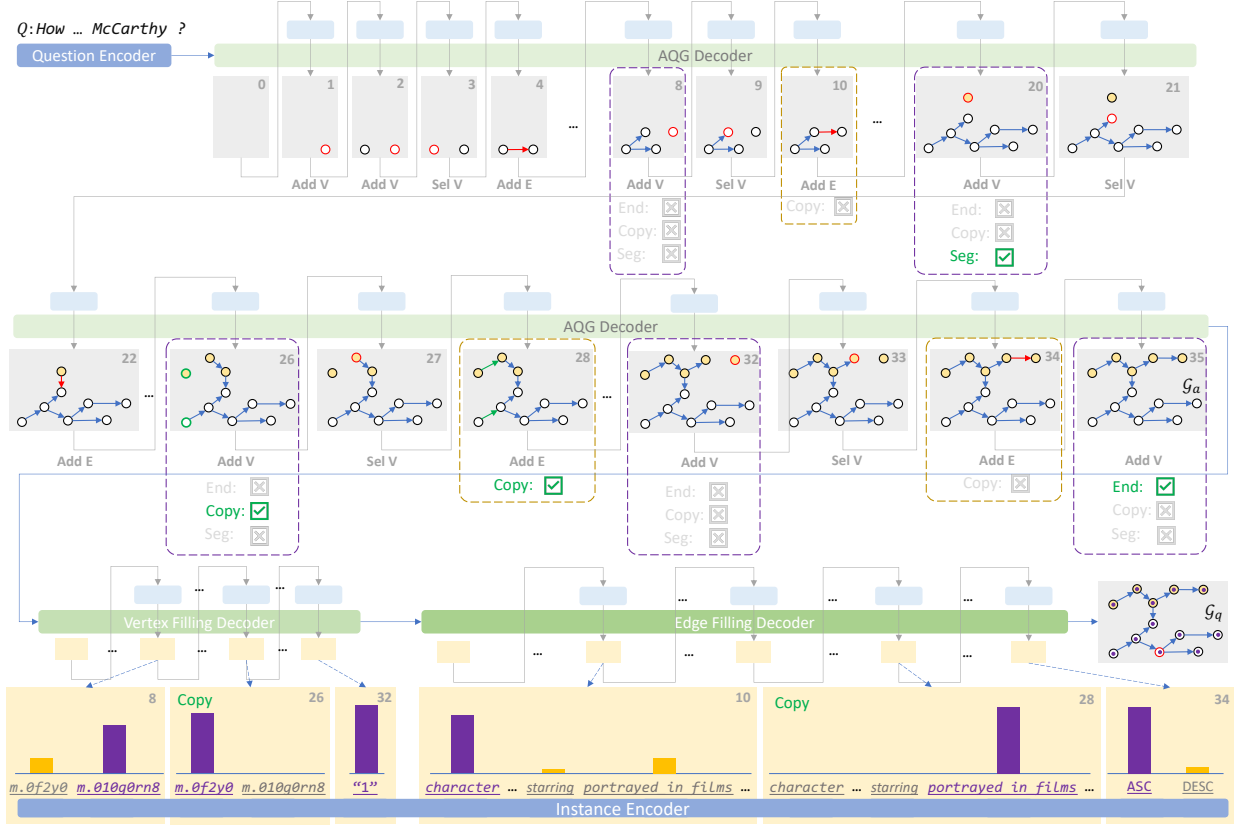


Fig. 5: Architecture of our proposed HGNet. Gray boxes illustrate the graph structure at each step of *Outlining*. Yellow boxes illustrate the bar charts of each instance at each step of *Filling*. Dotted boxes show some steps we focus.

step t of *Outlining*, we add a graph encoder to embed \mathcal{G}_{t-1} . In detail, HGNet consists of a question encoder, an instance encoder, a graph encoder, and three decoders.

6.1 Question Encoder & Instance Encoder

To capture the semantic information of question Q , we employ a Bi-LSTM as the question encoder. It converts the word embeddings of the tokenized Q to semantic vectors $\mathbf{Q} = [\mathbf{q}_1, \mathbf{q}_2, \dots, \mathbf{q}_M] \in \mathbb{R}^{M \times d}$, where M denotes the token number of Q and $\mathbf{q}_k \in \mathbb{R}^d$ is the vector of the k -th word.

The instance encoder is also set to a Bi-LSTM. For $i \in \mathcal{I}_c$, where $c \in \Psi \cup \Phi - \{\text{Ans}, \text{Var}\}$, its true name (e.g., `portrayed_in_films`) is tokenized and embedded, and then fed to the instance encoder. The returned semantic vectors are finally transformed with a max-pooling, to the vector representation $\mathbf{h}_i \in \mathbb{R}^d$. Here, to guarantee that Q and \mathcal{I} belong to the same semantic space, the parameters of the question and instance encoders are shared.

6.2 Graph Encoder

To aware of the structural feature of \mathcal{G}_{t-1} during *Outlining*, we apply a graph transformer [13] as the graph encoder. Concretely, at step t of *Outlining*, graph \mathcal{G}^{t-1} , in the form of vertex embeddings, edge embeddings, and an adjacency matrix, is fed to the graph encoder. Here, the embedding of each vertex/edge is represented by the corresponding class vector, which is randomly initialized. The graph encoder builds a pseudo graph by regarding both original vertices

and edges as the nodes linked by virtual edges. For each node, a k -layer multi-head attention [14] is performed to aggregate the information flow within its k -hop neighbors to update its own vector representation. The return consists of vertex vectors $\mathbf{V}^{t-1} = [\mathbf{v}_1, \mathbf{v}_2, \dots, \mathbf{v}_N]$, edge vectors $\mathbf{E}^{t-1} = [\mathbf{e}_1, \mathbf{e}_2, \dots, \mathbf{e}_{N-1}]$, and a graph vector representation $\mathbf{h}_{\mathcal{G}}^{t-1} \in \mathbb{R}^d$, where N denotes the vertex number of \mathcal{G}^{t-1} .

6.3 AQG Decoder

We employ a LSTM as the AQG decoder, which takes the last hidden states during encoding as the initial states. At each step t of *Outlining*, it integrates the context information of Q and the structural information of \mathcal{G}^{t-1} into a vector. Here, the context vector, denoted by $\mathbf{h}_{\mathcal{Q}}^t \in \mathbb{R}^d$, is calculated by an attention mechanism.

$$\mathbf{h}_{\mathcal{Q}}^t = \sum_{i=1}^M \text{softmax}(\mathbf{h}_{\mathcal{G}}^{t-1T} W_{\alpha} \mathbf{q}_i) \mathbf{q}_i \quad (3)$$

where $W_{\alpha} \in \mathbb{R}^{d \times d}$ is the trainable parameter matrix. Then, \mathbf{h}_{in}^t , the vector inputs to the AQG decoder, is obtained by

$$\mathbf{h}_{in}^t = \tanh(W_{in}[\mathbf{h}_{\mathcal{Q}}^t; \mathbf{h}_{\mathcal{G}}^{t-1}]) \quad (4)$$

where $W_{in} \in \mathbb{R}^{d \times 2d}$ is the affine transformation.

Outlining Argument Prediction The decoder returns vector $\mathbf{h}_{out}^t \in \mathbb{R}^d$ and the probabilities of *Outlining* arguments at step t are calculated as follows.

Arguments c_v^t and s_v^t of *AddVertex* are determined by

$$c_v^t = \arg \max_{c \in \Psi \cup \{\text{End}\}} \text{softmax}(\tanh(\mathbf{h}_{out}^t W_{av}) \cdot \mathbf{x}_c) \quad (5)$$

$$s_v^t = \begin{cases} 0 & t \leq 4 \\ s_v^{t-3} + \delta^t & t > 4 \end{cases} \quad (6)$$

$$\delta^t = \arg \max_{\delta \in \{0,1\}} \text{softmax}(\tanh(\mathbf{h}_{out}^t W_{\delta}) \cdot \mathbf{z}_{\delta}) \quad (7)$$

where $\mathbf{x}_c \in \mathbb{R}^d$ is the embedding of vertex class c , δ^t denotes a signal of whether switch the current segment, and $\mathbf{z}_{\delta} \in \mathbb{R}^d$ is the trainable signal embedding.

Argument u of *SelectVertex* is determined by

$$u = \arg \max_{u_i \in V^{t-1}} \text{softmax}(\tanh(\mathbf{h}_{out}^t W_{sv}) \cdot \mathbf{v}_i) \quad (8)$$

where $\mathbf{v}_i \in \mathbb{R}^d$ is the semantic vector of vertex u_i , obtained by the graph encoder.

Argument c_e of *AddEdge* is determined in a same manner of (5) while using another set of parameters.

Copy Mechanism We observe the query graph has some repeated vertices and edges sometimes, e.g., `m.0f2y0` and `portrayed_in_films` in Fig. 2b. Although they are the same on in semantic, SPARQL program repeat them for facilitating the access. We expect to recognize such vertices/edges during *Outlining* to further reduce the search space thence we adopt a *Copy Mechanism* on *AddVertex* and *AddEdge*. Specifically, for vertex v^t added by *AddVertex* at step t , the semantically equivalent vertex, denoted by \tilde{v}^t , is identified by

$$\tilde{v}^t = \arg \max_{v_i \in V^{t-1} \cup \{v_{\text{NONE}}\}} \text{softmax}(\tanh(\mathbf{h}_{out}^t W_{cv}) \cdot \mathbf{v}_i) \quad (9)$$

where \mathbf{v}_i is obtained by the graph encoder and v_{NONE} means that there is no such a vertex. For copying edges, a similar mechanism is performed on e^t of *AddEdge*.

6.4 Vertex Filling Decoder & Edge Filling Decoder

Consistent with the AQG decoder, both vertex filling decoder and edge filling decoder are LSTM and begin with the last hidden states of encoding. As mentioned in 5.2, we first vertex *Filling* decoding and then edge *Filling* decoding. Similar to *Outlining*, at step t of vertex/edge *Filling*, the context vector $\hat{\mathbf{h}}_{\mathcal{Q}}^t \in \mathbb{R}^d$ is computed by (3) with another parameters.

At each step t during *Filling*, the model needs to understand the semantic role of v^t/e^t to be filled in the entire graph, accordingly, $\hat{\mathbf{h}}_{in}^t$, the input to the vertex filling decoder is calculated by *Auxiliary Structural Encoding*.

$$\hat{\mathbf{h}}_{in}^t = \tanh(\hat{W}_{in}^v [\hat{\mathbf{h}}_{\mathcal{Q}}^t; \mathbf{h}_{g_a}; \mathbf{v}^t]) \quad (10)$$

where $\mathbf{h}_{g_a} \in \mathbb{R}^d$ is the vector representation of the AQG \mathcal{G}_a and $\mathbf{v}^t \in \mathbb{R}^d$ is the semantic vector of v^t . Both \mathbf{h}_{g_a} and \mathbf{v}^t are obtained by the graph encoder and hold auxiliary structural information. For edge filling decoder, the procedure is similar.

Filling Arguments Prediction The vertex/edge filling decoder returns a vector $\hat{\mathbf{h}}_{out}^t \in \mathbb{R}^d$, then the argument i_v^t of *FillVertex* is determined by

$$\hat{i}_v^t = \arg \max_{i \in \mathcal{I}_{cv}} \text{softmax}(\tanh(\hat{\mathbf{h}}_{out}^t W_v) \cdot \mathbf{h}_i) \quad (11)$$

$$i_v^t = \begin{cases} \hat{i}_v^t & \tilde{v}^t \neq \text{NONE} \\ \tilde{i}_v^t & \tilde{v}^t = \text{NONE} \end{cases} \quad (12)$$

where \mathbf{h}_i is the representation of instance i from the instance encoder, and \hat{i}_v^t is the filled instance of semantically equivalent vertex \tilde{v}^t . For operation *FillEdge*, argument i_e is determined in a similar manner.

During inference of HGNet, all decoders are enhanced by Beam Search [15] to avoid the local optimum.

Execution-Guided Strategy In general, a query graph must be illegal if its query result over the KG is empty. Motivated by this, we design an Execution-guided (EG) Strategy to avoid illegal graphs during edge *Filling*, in order to reduce error propagation. Algorithm 1 describes the detailed process. Briefly, at step t , for each candidate instance i , we first fill it to \mathcal{G}^t (line 7) and then execute the converted SPARQL over the KG (line 8-9). If the result is empty, i is masked by attaching $-\infty$ score for this step (line 13). Function TOSPARQL aims to convert \mathcal{G}_u into a equivalent SPARQL. In our proposed EG, the number of execution, denoted by η , has an upper bound $\sup(\eta) = (\mathcal{N} - 1)KY_{\mathcal{I}}$, where $Y_{\mathcal{I}}$ is the total number of the candidate instances, K is the beam size of each decoding step, and \mathcal{N} is the vertex number of

6.5 Discuss on Search Space

Let Y_o , Y_v , and Y_e denote the average size of the argument candidate set (sub-space) at each step of *Outlining*, *Vertex Filling*, and *Edge Filling*, respectively. Then, the total search space of generating query graph, approximated as the total number of beams, is $\hat{\mathcal{Y}} \approx (3\mathcal{N} - 1)KY_o + \mathcal{N}KY_v + (\mathcal{N} - 1)KY_e$, where beam size $K \leq 5$ and vertex number \mathcal{N} usually not exceeds 15. Generally, $Y_o, Y_v, Y_e \leq Y \approx 100$, where Y is the average number of one-hop relations between two KG entities, therefore, $\hat{\mathcal{Y}} \ll \mathcal{Y} \approx Y^L$ if $L > 3$. The beams are few enough to be embedded by the neural model during decoding thereby challenge 2 is solved.

6.6 Training

In our experiments, each training sample is a pair of an NLQ \mathcal{Q} and a gold SPARQL \mathcal{S}^+ . We train HGNet by supervised learning with teacher-forcing. During training, HGNet is optimized by maximizing the log-likelihood:

$$\begin{aligned} \mathcal{L} = & - \sum_{\mathcal{Q}} \sum_{t=1}^{|\mathcal{A}_o|} \sum_{a \in \mathcal{A}_o^t} \log P(\hat{a}^t = a | \mathcal{Q}) \\ & - \sum_{t=1}^{|\mathcal{A}_v|} \log P(\hat{b}^t = \mathcal{A}_v^t | \mathcal{Q}) - \sum_{t=1}^{|\mathcal{A}_e|} \log P(\hat{b}^t = \mathcal{A}_e^t | \mathcal{Q}) \end{aligned} \quad (13)$$

where \mathcal{A}_o , \mathcal{A}_v , and \mathcal{A}_e are the supervised signals of the three generation processes. They are obtained by a depth-first traversal on \mathcal{G}_q^+ , which is detailed in Appendix C. Here, \mathcal{G}_q^+ is the gold query graph transformed from \mathcal{S}^+ .

7 EXPERIMENTS

7.1 Experimental Setup

Our models are trained and evaluated over three KGQA datasets: **WebQuestionsSP**¹ (WebQSP) [7] contains 3,098

1. <http://aka.ms/WebQSP>

Algorithm 1 Execution-guided Decoding for HGNet

Require: Question \mathcal{Q} . Knowledge Graph \mathcal{K} . AQG \mathcal{G}_a . Candidate instance sets $\mathcal{I} = \{\mathcal{I}_x | x \in \Phi\}$. Beam size K . Edges to be filled $\{e_1, e_2, \dots, e_{N-1}\}$. Classes of edges $\{c_1, c_2, \dots, c_{N-1}\}$.

- 1: Initialize $t = 0$, beams $\mathcal{B} = \{(\mathcal{G}_a, 0)\}$
- 2: **while** $t < N - 1$ **do**
- 3: Set lived beams $\mathcal{B}_l = \emptyset$
- 4: **for** $(\mathcal{G}^t, s_{\mathcal{G}^t}) \in \mathcal{B}$ **do**
- 5: Set temporal beams $\hat{\mathcal{B}} = \emptyset$
- 6: **for** $i \in \mathcal{I}_{c_t}$ **do**
- 7: Set $\mathcal{G}_i^t = \text{COPY}(\mathcal{G}^t)$ and $\text{FILLEDEGE}(\mathcal{G}_i^t, e^t, i)$
- 8: Set $\mathcal{S}_i^t = \text{ToSPARQL}(\mathcal{G}_i^t)$
- 9: $\mathcal{R}_i = \text{EXECUTE}(\mathcal{S}_i^t, \mathcal{K})$
- 10: **if** $\mathcal{R}_i^t \neq \emptyset$ **then**
- 11: Set $s_{\mathcal{G}_i^t} = s_{\mathcal{G}^t} + \log P(\hat{i} = i | \mathcal{Q})$
- 12: **else**
- 13: Set $s_{\mathcal{G}_i^t} = s_{\mathcal{G}^t} - \infty$
- 14: **end if**
- 15: Set $\hat{\mathcal{B}} = \hat{\mathcal{B}} \cup \{(\mathcal{G}_i^t, s_{\mathcal{G}_i^t})\}$
- 16: **end for**
- 17: Set $\mathcal{B}_l = \mathcal{B}_l \cup \text{TOPK}(\hat{\mathcal{B}}, K)$
- 18: **end for**
- 19: **if** $\mathcal{B}_l = \emptyset$
- 20: **break**
- 21: **end if**
- 22: Set $\mathcal{B} = \text{TOPK}(\mathcal{B}_l, K)$
- 23: $t = t + 1$
- 24: **end while**
- 25: **return** $\text{TOPK}(\mathcal{B}, 1)$

training and 1,639 testing NLQs that are answerable against Freebase 2015-08 release. Most NLQs require up to 2-hop reasoning from the KG with constraints of entities and time. **LC-QuAD²** [6] is a gold standard complex question answering benchmark over DBpedia 2016-04 release, having 3,500 training, 500 validation, and 1,000 testing pairs of NLQ and SPARQL queries. It contains three types of NLQs: selection, boolean, and count. **ComplexWebQuestions³** (CWQ) [2] is one of the hardest KGQA benchmarks currently and each NLQ corresponds to an executable SPARQL query. It has 27,623 training, 3,518 validation, and 3,531 testing pairs of NLQ and SPARQL queries. The NLQs require up to 4-hop reasoning with some complicated constraints of comparison, ordinary and nested queries.

For all datasets, we adopt Precision, Recall, F1-score, and Hit@1 as the evaluation metrics, which are consistent with the previous work [10], [12], [16], [17]. We also evaluate our approach in terms of AQG Accuracy (\mathcal{G}_a Acc.) and Query Graph Accuracy (\mathcal{G}_q Acc.), which directly reflects the performance on semantic understanding.

Implementation Details In our experiments, all word embeddings are initialized with 300-d pre-trained word embeddings using GloVe [18]. The hyperparameters of HGNet are set as follows: (1) The dimension of all the semantic vectors, i.e., d_h , is set to 256; (2) The layer number of all the Bi-LSTMs is set to 1 and the layer number of the graph transformer is

TABLE 1: Recall of candidates instances.

Class	CWQ	LC-QuAD	WebQSP
Type	99.65	97.80	-
Rel	95.24	95.32	93.90
Val	89.63	-	94.82

TABLE 2: Average Hit@1/F1-score on CWQ, LCQ, and WSP.

Approach	CWQ	LC-QuAD	WebQSP
STAGG [1]	-/-	-/69.0	-/67.0
HR-BiLSTM [8]	33.3/31.2	-/70.0	-/68.0
GRAFT-Net [9]	30.1/26.0	-/-	67.8/62.8
KBQA-GST [19]	39.3/36.5	-/-	68.2/67.9
PullNet [10]	45.9/-	-/-	68.1/-
Slot-Matching [11]	-/-	-/71.0	-/70.0
AQGNet [17]	-/-	-/74.8	-/-
DAM [20]	-/-	-/72.0	-/70.0
QGG [21]	44.1/40.4	-/-	-/74.0
NSM+h [12]	48.8/44.0	-/-	74.3/67.4
HGNet	65.3/64.9	76.0/75.1	70.6/70.3

set to 3; (3) The learning rate is set to 2×10^{-4} ; (4) The size of each beam is set to 5 for CWQ and 7 for LC-QuAD and WebQSP. (5) The batch size is set to 16. (6) For class Rel and Type, the numbers of candidate instances are set to 50 and 3, respectively. (7) The beam sizes of all decoding are set to 5. All our code are publicly available⁴.

Performance of Candidate Instance Collection Table 1 gives the recall of candidates for Type, Rel, and Val. Some classes of Ent, Ord, Cmp, and Agg are not shown because they have recall of 100%. In addition, WebQSP has no Type instances and LC-QuAD has no Val instances.

Approaches for Comparison We first compared our approach with the following existing approaches. STAGG [1], HR-BiLSTM [8], and DAM [20] establishes query graph generation pipelines that predicts topic entity, core relation chain, and constraints in turn. Slot-Matching [11] ranks query graphs by a slot attention mechanism. AQGNet [17] is our previous work that leverages AQG to achieve state-of-the-art on LC-QuAD. However, it is still based on ranking consequently suffers from the challenge 1 and 2. There is a lack of supervised approaches for comparison on CWQ due to the challenges. Therefore, we have to compare with the weakly supervised approaches including KBQA-GST [19], QGG [21], GRAFT-Net [9], PullNet [10], and NSM+h [12]. Although these approaches abandon SPARQL annotation, they still extract paths or sub-graphs from the KG as the signals to apply multi-hop reasoning.

7.2 Overall Results

The experimental results are reported in Table 2. On WebQSP, our HGNet ranks second only to NSM+h [12] and QGG [21] in terms of hit@1 and F1-score, respectively. On both LC-QuAD and CWQ, HGNet achieves the state-of-the-art in terms of both hit@1 and F1-score. In particular, on the hardest CWQ, HGNet significantly improves the performance by 16.5% and 20.9% in terms of hit@1 and F1-score, respectively. Besides, our approach outperforms all the existing ranking-based approaches [11], [17] on all the datasets.

2. <https://figshare.com/projects/LC-QuAD/21812>

3. <https://www.tau-nlp.org/compwebq>

4. <https://github.com/Bahua/HGNet>

TABLE 3: Experimental results for comparison with baselines.

Baselines	CWQ					LC-QuAD					WebQSP				
	\mathcal{G}_q	Acc.	Prec.	Rec.	F1	\mathcal{G}_q	Acc.	Prec.	Rec.	F1	\mathcal{G}_q	Acc.	Prec.	Rec.	F1
S-Ranking	-	-	-	-	-	54.75	65.89	75.30	69.53	62.58	70.82	80.50	71.52		
O-Ranking	-	-	-	-	-	60.80	75.54	74.95	74.81	61.95	70.30	74.32	70.89		
BART	-	27.97	28.30	27.62	-	-	48.01	49.19	47.62	-	53.20	56.17	53.49		
NHGG	47.89	59.09	63.15	59.12	-	27.10	46.93	48.36	46.12	54.59	60.74	64.22	60.68		
HGNet	51.68	65.27	68.44	64.95	-	60.90	75.82	75.22	75.10	62.63	70.22	74.38	70.61		

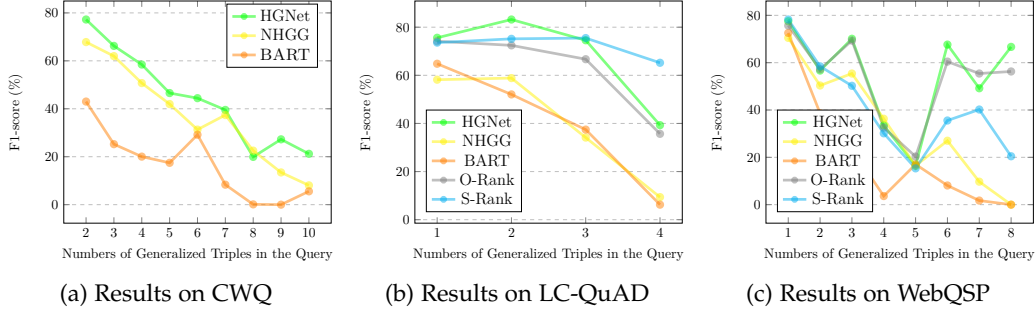


Fig. 6: F1-score on different complexity levels of questions.

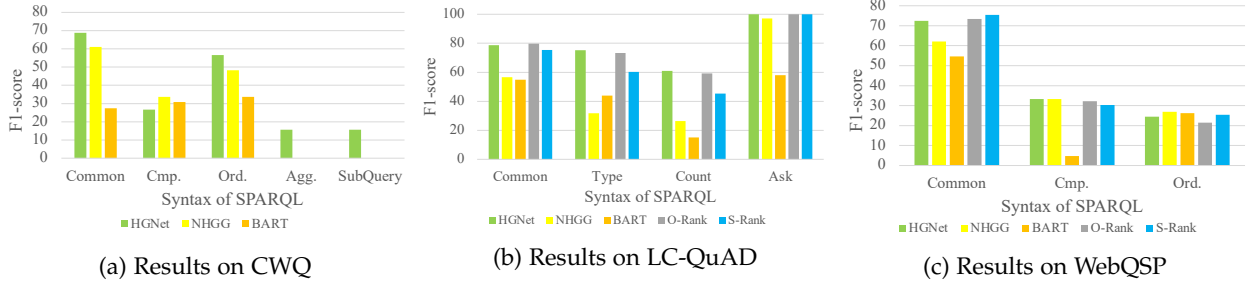


Fig. 7: F1-score on different types of SPARQL syntax.

The performance of STAGG [1], HR-BiLSTM [8], and DAM [20] is limited by the error propagation of the pipeline. Slot-Matching [11] and AQGNet [17] can not handle CWQ owing to challenge 2. The remain weakly supervised approaches [9], [10], [12], [19], [21] have poor performance on CWQ because they are unable to learn the semantic information in various constraints without detailed SPARQL supervision. Our query graph provides a paradigm for using the complicated SPARQL to train the model. Furthermore, our HGNet integrates the structural constraint to the generation process by hierarchical autoregressive decoding, thus performing well on complex benchmarks.

7.3 Detail Results and Analysis

7.3.1 Comparison with Baselines of Supervised Learning

We arrange several strong baselines, which are based on supervised learning, for further comparison.

STAGG+Ranking (S-Rank) first generates candidate query graphs by STAGG [1] and then ranks the candidates with CompQA [22], which is a strong ranking model.

Outlining+Ranking (O-Rank) generates AQG \mathcal{G}_a by *Outlining* and subsequently produces the candidate graphs by enumerating the combination of instances to fill \mathcal{G}_a . Thereafter, the candidates are also ranked with CompQA [22].

BART [23], which is a strong pre-trained sequence-to-sequence model, directly treats the problem as a conventional machine translation task from NLQ to SPARQL.

Non-hierarchical Graph Generation (NHGG) integrates *Outlining* and *Filling* into one procedure. For *AddVertex* and *AddEdge*, the model directly predicts instances instead of classes. In this way, the query graph can be completed by only one decoding process without *Filling* operations.

The experimental results are shown in Table 3. S-Rank and O-Rank have no results on CWQ because both of them can not bear challenge 2, even if the search space of the latter has been reduced by the AQG. In addition, BART has no result of \mathcal{G}_q Acc because it merely generates SPARQL. Note that our HGNet has a better \mathcal{G}_q than S-Ranking on WebQSP while worse in Prec, Rec, and F1. This is due to the problem of pseudo query graphs [12], i.e., S-Rank obtains some incorrect query graphs that have wrong semantic yet coincidentally retrieve the correct answers. It is absolutely not what a good system expects, thus we focus on the performance on \mathcal{G}_q Acc. The results demonstrate that our HGNet performs better than all the baselines in terms of \mathcal{G}_q Acc on all datasets. Even though compared with *O-Ranking* benefiting also from structure constraint, HGNet is still competitive (+0.1% on LC-QuAD, +0.05% on WebQSP). It proves that our *Filling* process is comparable to *Ranking*

TABLE 4: Experimental results of ablation test.

Settings	CWQ			LC-QuAD			WebQSP		
	\mathcal{G}_a Acc.	\mathcal{G}_q Acc.	F1	\mathcal{G}_a Acc.	\mathcal{G}_q Acc.	F1	\mathcal{G}_a Acc.	\mathcal{G}_q Acc.	F1
HGNet	66.96	51.68	64.95	78.00	60.90	75.10	79.91	62.63	70.61
– Graph Encoder	61.03	47.75	61.77	70.70	56.70	70.78	73.42	58.64	66.82
– Auxiliary Encoding	66.90	49.22	62.81	78.10	60.00	73.63	78.91	60.45	68.41
– Copy	66.35	50.32	65.97	76.70	52.90	71.00	79.23	63.76	71.44
– EG	69.58	44.11	50.96	76.90	32.30	35.91	80.16	57.33	61.88

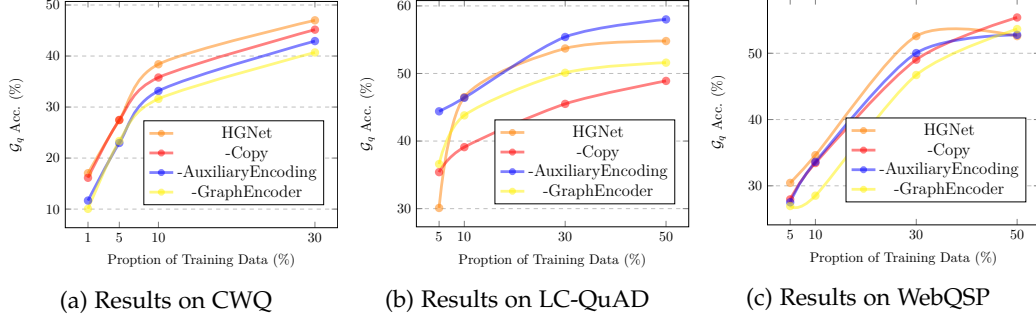


Fig. 8: Accuracy of query graph building with different proportions of training data.

on performance while significantly reducing space cost. In terms of \mathcal{G}_q , our substantial improvement (3.7%, 33.8%, 8.0%) on NHGG reveals the necessity of the hierarchical procedure. Here, the extremely poor performance of NHGG on LC-QuAD is mainly owed to considerable type in this benchmark. Without *Outlining*, it is hard for the model to select the only correct type from the total candidate instance pool containing all categories. BART does not work well on all datasets, especially CWQ because it ignores the structural feature of SPARQL while flattening it as a sequence of tokens. In this manner, any wrong token results in the failure of the entire SPARQL.

7.3.2 Performance on Different Complexity and Types

To further analyze the performance on complex NLQs, we define that a complex level of an NLQ is the edge number of the corresponding query graph since more edges intuitively lead to more semantic information. Fig. 6 shows the F1-scores on different levels. HGNet achieves the best performance on almost all the levels of NLQs. For the hardest CWQ, compared with BART and NHGG, the improvements brought by HGNet are more significant on the NLQs above level 5. It highlights the contribution of hierarchical graph generation on complex NLQs once more. In addition, on the levels within 4, HGNet is also competitive with the strong ranking-based approaches. We observed that, on WebQSP, the fluctuations of each approach are relatively large because the amount of high-level NLQs in this dataset is so small that any little error results in a great gap.

We also evaluate the performance of the approaches on dealing with various SPARQL syntax and the experimental results are shown in Table 7, where `Common` denotes the SPARQL that has only relation triples. Both benefiting from *Outlining* process, the F1-scores of O-Rank and HGNet are close on different syntax types of LC-QuAD and WebQSP. However, on CWQ, except `Cmp`, HGNet has significant advantages on handling `ORDER BY` clauses (`Ord.`), aggregation

functions (`Agg.`), and nest queries, especially on the last two types, where neither NHGG nor BART is helpless.

7.3.3 Ablation Test

To explore the contributions of each component of our HGNet, we compare the performance of the model of the following settings:

- **Graph Encoder** In *Outlining*, we remove the graph encoder and modify (4) to $\mathbf{h}_{in}^t = \tanh(W_{in}[\mathbf{h}_Q^t; \mathbf{h}_{out}^{t-1}])$.
- **Auxiliary Encoding** In *Filling*, we remove the auxiliary structural encoding and modify (10) to $\hat{\mathbf{h}}_{in}^t = \tanh(\hat{W}_{in}^v \hat{\mathbf{h}}_Q^t)$.
- **Copy** During *Filling* we remove the copy mechanism and modify (12) to $i_v^t = i_v^t$.
- **EG** We remove the Execution-guided strategy thereby performing edge *Filling* by the model prediction only.

Table 4 shows \mathcal{G}_a Acc, \mathcal{G}_q Acc, and F1-score of the ablations. By removing the graph encoder, \mathcal{G}_a Acc declines averagely 7% on all datasets. It evidences that the complete structural information of the previous-step graph is essential for *Outlining*. Discarding the auxiliary structural encoding results in drops in terms of \mathcal{G}_q Acc for all datasets (-2.5%, -0.9%, -4.0%), while a little increment in terms of \mathcal{G}_a Acc for LC-QuAD (0.1%). A possible cause is that the auxiliary encoding might influence original information flow for structure prediction. In contrast, the copy mechanism plays a significant role on \mathcal{G}_q Acc for LC-QuAD because a considerable number of SPARQLs have repeated relations. The removal of EG bring absolute drops (-7.5%, -28.6%, -5.3%) in terms of \mathcal{G}_q Acc on all datasets. It proves that KG is efficient for query graph disambiguation. Compared with LC-QuAD, the contribution of EG on CWQ and WebQSP is smaller because LC-QuAD are based on DBpedia, suffering from the conflict of property and ontology.

7.3.4 Few-shot Performance

To explore the few-shot performance of HGNet, we train the model with different sizes of training data ($\{1\%, 5\%$,

TABLE 5: Major causes for failures and descriptions on the test set of CWQ.

Cause of Error	Description	Proportion
Comparison Constraint	The <code>FILTER</code> -clauses that denote a comparison relationship in S_p are redundant or missing.	18%
Ordinal Constraint	The <code>ORDER BY</code> -clause in S_p is missing or its variable object is incorrect.	2%
Relation Triple	The relation triples in S_p are redundant or missing, or their topology is incorrect.	40%
Empty SPARQL	The <code>WHERE</code> -clause of S_p does not have any relation triples or <code>FILTER</code> -clauses.	22%
Entity	The entities are filled into the wrong entity slots of the AQG when there are multiple entities in S_p .	4%
Relation	The incorrect relation instances are filled into the relation slots of the AQG.	12%
Operator & Value	Some operators and values in the <code>Filter</code> -clauses are incorrect.	12%

10%, 30%} for CWQ, {5%, 10%, 30%, 50%} for LC-QuAD and WebQSP). The results are reported in Fig. 8. For each size of CWQ, the complete HGNet equipped with all the components maintains optimal performance and has steady improvements over other ablation settings. The major reason for its poor performance on the 5% setting of LC-QuAD is that the training data is too little (only 175 NLQs) for the model to learn to generate structures and copy instances simultaneously. Yet WebQSP has no such cases because most of its SPARQL programs are simple enough to learn.

7.3.5 Error Analysis

To understand the source of errors, we randomly analyze 100 failed examples of HGNet on the test set of CWQ. We summarize several major causes for failures, which are shown in TABLE 5. The top exhibits the errors in structure prediction and the bottom the errors in instance prediction. Notice that the sum of all proportions exceeds 100% because one failure could be due to multiple causes. The structure errors are mainly reflected in the redundancy, missing, and the wrong topology of the relation triples. Sometimes, EG abandons all the beams owing to the conflict of predicted structure and candidate instances in the KG, thereby producing empty SPARQL. The current bottleneck restricting performance is still the incomplete semantic understanding of the NLQ. Some relations often do not have any explicit mention only requiring domain knowledge to be recognized. The pre-trained models fusing domain knowledge could be a promising direction.

8 RELATED WORK

Knowledge Graph Question Answering The KGQA task aims to provide crisp answers to NLQs. Generally, the solutions of KGQA can be mainly divided into three categories. The first one is based on Semantic Parsing, which translates NLQs into logical forms. Our HGNet belongs to this category. Early works handle the problem by paraphrasing or pre-defined templates [24], [25]. With the development of advanced deep learning, later approaches [1], [8], [16], [20], [26], [27] establish complicated pipelines by neural networks. Hu et al. [16] define four operations to perform a state-transition generation process to build query graphs. Different from our proposed operations, theirs rely on the manually defined rules to identify the conditions on whether to perform the operation. Recent approaches simplify pipeline into query graph ranking [11], [17], [22]. The major difference between our approach and previous approaches is that we propose a hierarchical generation framework to leverage the structural constraint to narrow the search space. Furthermore, our approach does not need

predefined templates and conditions. The second category is based on Information Retrieval, which does not product logical form but selects candidate answers first and then rank them by various methods [28], [29], [30]. The third category depends on Multi-hop Reasoning, which intends to employ classical approaches (e.g., Key-Value Memory Network and Graph Convolution Network) to conduct a multi-hop reasoning within the KG [9], [10], [31], [32].

Intermediate Representations in KGQA Traditional approaches [24], [25] leverage λ -DCS, which can be regarded as a syntax tree, as intermediate representation (IR) to represent the meaning of questions. Yih et al. [1] propose to represent SPARQL by a query graph, which consists of a topic entity, a core relation chain, and constraint nodes. It is the first time that treats represent the logical form from the perspective of graphs. However, their query graph is too coarse-grained to more complicated SPARQL syntax like nested queries because the complicated SPARQL syntax can not be represented merely by the relation chain attached constraint nodes. Different from it, our redefined query graph regards entities, values, types, relations, and built-in properties, as the true vertex or edges, thereby has stronger representation capability.

Grammar-based Decoding The goal of Grammar-based Decoding is to generate a top-down grammar rule at each step of autoregressive decoding and receives more and more attention in Text-to-SQL [3], [4], [5], which is another semantic parsing task, that is, our generation process depends on graph grammar rather than top-down grammar. It is typically difficult for the model to directly forecast (outline) the entire structure from the root node, while our approach is not limited by tree hierarchy thus could add new partial semantic information to the graph at any time of *Outlining*.

9 CONCLUSION

In this paper, we presented a new approach for complex knowledge graph question answering (KGQA), which transforms the NLQ into executable query graphs. We initially redefine the query graph grammar, and subsequently, propose a new hierarchical autoregressive generation model. It first outlines the query graph structure and then fills the instances into the structure thereby completing the query graph. The redefined query graph grammar is able to represent the complicated SPARQL syntax, making it possible to handle complex NLQs. Benefiting from the structure constraint provided by the hierarchical generation procedure, our model greatly reduces the search space of candidates meanwhile avoid local ambiguity. The experimental results prove that our model achieved superior results than the existing approaches, especially on complex

NLQs. In future work, we will try to enhance the model with pre-trained language models to leverage the knowledge from mass corpus. We will also try to port the model to the weakly supervised condition of only question-answer pairs.

REFERENCES

- [1] W. Yih, M. Chang, X. He, and J. Gao, "Semantic parsing via staged query graph generation: Question answering with knowledge base," in *ACL*, 2015, pp. 1321–1331.
- [2] A. Talmor and J. Berant, "The web as a knowledge-base for answering complex questions," in *NAACL*, 2018, pp. 641–651.
- [3] T. Yu, M. Yasunaga, K. Yang, R. Zhang, D. Wang, Z. Li, and D. R. Radev, "Syntaxsqlnet: Syntax tree networks for complex and cross-domain text-to-sql task," in *EMNLP*, 2018, pp. 1653–1663.
- [4] J. Guo, Z. Zhan, Y. Gao, Y. Xiao, J. Lou, T. Liu, and D. Zhang, "Towards complex text-to-sql in cross-domain database with intermediate representation," in *ACL*, 2019, pp. 4524–4535.
- [5] B. Wang, R. Shin, X. Liu, O. Polozov, and M. Richardson, "RAT-SQL: relation-aware schema encoding and linking for text-to-sql parsers," in *ACL*, 2020, pp. 7567–7578.
- [6] P. Trivedi, G. Maheshwari, M. Dubey, and J. Lehmann, "Lc-quad: A corpus for complex question answering over knowledge graphs," in *ISWC*, vol. 10588, 2017, pp. 210–218.
- [7] W. Yih, M. Richardson, C. Meek, M. Chang, and J. Suh, "The value of semantic parse labeling for knowledge base question answering," in *ACL*, 2016.
- [8] M. Yu, W. Yin, K. S. Hasan, C. N. dos Santos, B. Xiang, and B. Zhou, "Improved neural relation detection for knowledge base question answering," in *ACL*, 2017, pp. 571–581.
- [9] H. Sun, B. Dhingra, M. Zaheer, K. Mazaitis, R. Salakhutdinov, and W. W. Cohen, "Open domain question answering using early fusion of knowledge bases and text," in *EMNLP*, 2018, pp. 4231–4242.
- [10] H. Sun, T. Bedrax-Weiss, and W. W. Cohen, "Pullnet: Open domain question answering with iterative retrieval on knowledge bases and text," in *EMNLP*, 2019, pp. 2380–2390.
- [11] G. Maheshwari, P. Trivedi, D. Lukovnikov, N. Chakraborty, A. Fischer, and J. Lehmann, "Learning to rank query graphs for complex question answering over knowledge graphs," in *ISWC*, vol. 11778, 2019, pp. 487–504.
- [12] G. He, Y. Lan, J. Jiang, W. X. Zhao, and J. Wen, "Improving multi-hop knowledge base question answering by learning intermediate supervision signals," in *WSDM*, 2021, pp. 553–561.
- [13] R. Koncel-Kedziorski, D. Bekal, Y. Luan, M. Lapata, and H. Hajishirzi, "Text generation from knowledge graphs with graph transformers," in *NAACL*, 2019, pp. 2284–2293.
- [14] A. Vaswani, N. Shazeer, N. Parmar, J. Uszkoreit, L. Jones, A. N. Gomez, L. Kaiser, and I. Polosukhin, "Attention is all you need," in *NIPS*, 2017, pp. 5998–6008.
- [15] S. Wiseman and A. M. Rush, "Sequence-to-sequence learning as beam-search optimization," *CoRR*, vol. abs/1606.02960, 2016.
- [16] S. Hu, L. Zou, and X. Zhang, "A state-transition framework to answer complex questions over knowledge base," in *EMNLP*, 2018, pp. 2098–2108.
- [17] Y. Chen, H. Li, Y. Hua, and G. Qi, "Formal query building with query structure prediction for complex question answering over knowledge base," in *IJCAI*, 2020, pp. 3751–3758.
- [18] J. Pennington, R. Socher, and C. D. Manning, "Glove: Global vectors for word representation," in *ACL*, 2014, pp. 1532–1543.
- [19] Y. Lan, S. Wang, and J. Jiang, "Knowledge base question answering with topic units," in *IJCAI*, 2019, pp. 5046–5052.
- [20] Y. Chen and H. Li, "DAM: transformer-based relation detection for question answering over knowledge base," *Knowl. Based Syst.*, vol. 201–202, p. 106077, 2020.
- [21] Y. Lan and J. Jiang, "Query graph generation for answering multi-hop complex questions from knowledge bases," in *ACL*, 2020, pp. 969–974.
- [22] K. Luo, F. Lin, X. Luo, and K. Q. Zhu, "Knowledge base question answering via encoding of complex query graphs," in *EMNLP*, 2018, pp. 2185–2194.
- [23] M. Lewis, Y. Liu, N. Goyal, M. Ghazvininejad, A. Mohamed, O. Levy, V. Stoyanov, and L. Zettlemoyer.
- [24] J. Berant, A. Chou, R. Frostig, and P. Liang, "Semantic parsing on freebase from question-answer pairs," in *EMNLP*, 2013, pp. 1533–1544.
- [25] J. Berant and P. Liang, "Semantic parsing via paraphrasing," in *ACL*, 2014, pp. 1415–1425.
- [26] S. Hu, L. Zou, J. X. Yu, H. Wang, and D. Zhao, "Answering natural language questions by subgraph matching over knowledge graphs," *IEEE Trans. Knowl. Data Eng.*, vol. 30, no. 5, pp. 824–837, 2018.
- [27] J. Ding, W. Hu, Q. Xu, and Y. Qu, "Leveraging frequent query substructures to generate formal queries for complex question answering," in *EMNLP*, 2019, pp. 2614–2622.
- [28] X. Yao and B. V. Durme, "Information extraction over structured data: Question answering with freebase," in *ACL*, 2014, pp. 956–966.
- [29] A. Bordes, S. Chopra, and J. Weston, "Question answering with subgraph embeddings," in *EMNLP*, 2014, pp. 615–620.
- [30] L. Dong, F. Wei, M. Zhou, and K. Xu, "Question answering over freebase with multi-column convolutional neural networks," in *ACL*, 2015, pp. 260–269.
- [31] A. H. Miller, A. Fisch, J. Dodge, A. Karimi, A. Bordes, and J. Weston, "Key-value memory networks for directly reading documents," in *EMNLP*, 2016, pp. 1400–1409.
- [32] Y. Zhang, H. Dai, Z. Kozareva, A. J. Smola, and L. Song, "Variational reasoning for question answering with knowledge graph," in *AAAI*, 2018, pp. 6069–6076.

APPENDIX A

PRE-PROCESSING OF TRANSFORMING SPARQL TO QUERY GRAPH

A.1 Constraint of Temporal Interval

We observe that some SPARQL programs have the sub queries that provide temporal intervals as constraints. Fig. 10a shows such a SPARQL program \mathcal{S} in CWQ. It has two sub-queries, namely \mathcal{S}_1 (yellow box) and \mathcal{S}_2 (orange box), which aims to query temporal intervals $[?from, ?to]$ and $[?pfrom, ?pto]$. Here, $?from$ and $?to$ respectively denote the start time and end time of being *President* (m.060c4) for *Woodrow Wilson* (m.083q7). $?from$ and $?to$ respectively denote the start time and end time of the *Military Conflict* (m.02h76fz). \mathcal{S}_1 and \mathcal{S}_2 are linked by a *FILTER* clause (green box). The clause describes the constraint that period $[?from, ?to]$ is during period $[?pfrom, ?pto]$.

Such constraints of temporal intervals typically result in a problem: the corresponding query graph \mathcal{G}_q does not follow Property 2 because it has the following generalized cycle path (red path in Fig. 10) without considering the direction, thereby can not be handled by our generation framework.

$$\begin{aligned} ?x(0) \xrightarrow{\text{start_date}} ?from(1) \xrightarrow{\geq} ?pfrom(2) \xleftarrow{\text{from}} ?y1(2) \\ \xrightarrow{\text{to}} ?pto(2) \xleftarrow{\leq} ?to(1) \xleftarrow{\text{end_date}} ?x(0) \end{aligned}$$

We propose a simple but efficient strategy to avoid the cycle path produced by temporal intervals. Initially, we retrieve all the temporal intervals in the SPARQL program by checking the *FILTER* clauses because a temporal variables are always in *FILTER* clauses and connected with the described variable (e.g., $?x$) along a relation r (e.g., *start_date*). We let $p = [t_{st}, t_{ed}]$ denotes the temporal interval, r_{st} and r_{ed} denote the two relations connected to t_{st} and t_{ed} , respectively. They are combined to a new relation r_p . In addition, to describe the comparison relationship between temporal intervals, we define the following two new operators:

- **DURING:** $\forall p^1 = [t_{st}^1, t_{ed}^1], \forall p^2 = [t_{st}^2, t_{ed}^2], p^1 \text{ DURING } p^2$ represents $t_{st}^1 \geq t_{st}^2$ AND $t_{ed}^1 \leq t_{ed}^2$.
- **OVERLAP:** $\forall p^1 = [t_{st}^1, t_{ed}^1], \forall p^2 = [t_{st}^2, t_{ed}^2], p^1 \text{ OVERLAP } p^2$ represents $t_{st}^1 \leq t_{ed}^2$ AND $t_{ed}^1 \geq t_{st}^2$.

In this way, the cycle in Fig. 10 is converted to the following chain.

$$?x(0) \xrightarrow{\text{start_date}} ?p(1) \xrightarrow{\text{DURING}} ?p1(2) \xleftarrow{\text{from}} ?y1(2)$$

where both $?p(1)$ and $?p1(2)$ are the temporal intervals, *from\$\$\$to* and *start_date\$\$\$end_date* are the combined relations. Fig. 11 shows \mathcal{S} and the new query graph after combining. By the observation, we found that only two kinds of relation pairs are used to describe temporal intervals, namely $(x.\text{from}, x.\text{to})$ and $(x.\text{start_date}, x.\text{end_date})$, where x is the domain prefix. Therefore, we collect all such relations to combine each pair of them into a new relation. In the first stage of our proposed approach, these new relations are also

Algorithm 2 Supervised Signal Building for HGNet

Require: A query graph $\mathcal{G}_q = (V_q, E_q, \Psi_q, \Phi_q, S_q)$.

```

1: Initialize Outlining supervised signals  $\mathcal{A}_o = []$ , vertex
   Filling supervised signals  $\mathcal{A}_v = []$ , edge Filling super-
   vised signals  $\mathcal{A}_e = []$ .
2: function DEPTHFIRSTTRAVERSAL( $u$ )
3:   for vertex  $v \in V_q - \{u\}$  do
4:     Set edge  $e^+ = \langle u, v \rangle, e^- = \langle v, u \rangle$ ,
5:     Set copied vertex  $\hat{v} = \text{GETCOPY}(v)$ 
6:     Set copied edge  $\hat{e}^+ = \text{GETCOPY}(e^+), \hat{e}^- =$ 
        $\text{GETCOPY}(e^-)$ 
7:     Set vertex instance  $i_v = \text{GETINSTANCE}(v)$ 
8:     Set edge instance  $i_{e^+} = \text{GETINSTANCE}(e^+),$ 
        $i_{e^-} = \text{GETINSTANCE}(e^-)$ 
9:     if  $e^+ \in E_q$  then
10:       $\mathcal{A}_o.\text{APPEND}([c_v, s_v, \hat{v}])$ 
11:       $\mathcal{A}_o.\text{APPEND}([u])$ 
12:       $\mathcal{A}_o.\text{APPEND}([c_{e^+}, \hat{e}^+])$ 
13:       $\mathcal{A}_v.\text{APPEND}(i_v)$ 
14:       $\mathcal{A}_e.\text{APPEND}(i_{e^+})$ 
15:      DEPTHFIRSTTRAVERSAL( $v$ )
16:     else if  $e^- \in E_q$  then
17:       $\mathcal{A}_o.\text{APPEND}([c_v, s_v, \hat{v}])$ 
18:       $\mathcal{A}_o.\text{APPEND}([u])$ 
19:       $\mathcal{A}_o.\text{APPEND}([c_{e^-}, \hat{e}^-])$ 
20:       $\mathcal{A}_v.\text{APPEND}(i_v)$ 
21:       $\mathcal{A}_e.\text{APPEND}(i_{e^-})$ 
22:      DEPTHFIRSTTRAVERSAL( $v$ )
23:     end if
24:   end for
25: end function
26:  $\mathcal{A}_o.\text{APPEND}([Ans, 0, NONE])$ 
27:  $\mathcal{A}_v.\text{APPEND}(NONE)$ 
28: DEPTHFIRSTTRAVERSAL( $u_{Ans}$ )
29:  $\mathcal{A}_o.\text{APPEND}([End, 0, NONE])$ 
30: return  $\mathcal{A}_o, \mathcal{A}_v, \mathcal{A}_e$ 

```

added to the relation pool with the normal relations, which are all fed to the relation ranker to select candidate instances. During inference, HGNet could fill them into the edge slots to build the query graph. Finally, when the completed query graph is converted to the SPARQL program, such combined relations are split into the pair of normal relations, in order to restore the cycle path by simple inverse rules.

A.2 Sub-query with $?x$ Intention

The SPARQL program \mathcal{S} in Fig. 11 still has a problem that answer $?x$ does not only appear in the *SELECT*-clauses of the main query but also in that of sub-query \mathcal{S}_1 (yellow). The problem causes that the segment number of $?x$ is hard to determine. In \mathcal{G}_q , segment 1 (yellow) corresponding to \mathcal{S}_1 is divided into multiple parts by $?x(0)$ (white) belonging to segment 0. Although it does not influence the generation process of HGNet, it is difficult to restore the final generated query graph to \mathcal{S} due to the broken of the segment.

To solve this problem, we propose to merge such the sub-query with $?x$ intention (i.e., \mathcal{S}_2) with the main query before transforming SPARQL to the query graph. The obtained new SPARQL $\hat{\mathcal{S}}$ is shown in Fig. 12. In fact, \mathcal{S} and $\hat{\mathcal{S}}$ are

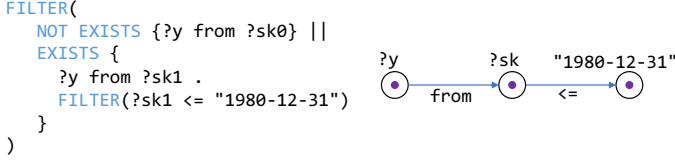


Fig. 9: An example of EXISTS clause in FILTER clause.

semantic equivalent and have identical retrieved answers, while the query graph of the latter retains complete segments so that can be restored to an executable SPARQL program easily.

A.3 EXISTS Clause in FILTER Clause

In our used datasets, the EXISTS clause usually appears in FILTER clause. Considering the example in the left of Fig. 9, a SPARQL sub-program describes a constraint \mathcal{C} that the start time of $?y$ is less than 1980-12-31. Here, EXISTS aims to represent the case that $?y$ have the start time and NOT EXISTS aims to deal with that $?y$ does not have the start time. || is used for the conjunction of the two cases above to prevent execution failure of the SPARQL. Actually, the two EXISTS clauses are not associated with the semantic information of the NLQ, while are merely the underlying implementation of SPARQL and the KG. Therefore, as the intermediate representation, our query graph should not represent such EXISTS for eliminating the gap between NLQ and SPARQL. The query graph needs only to describe the constraint \mathcal{C} , which is shown in the right of Fig. 9.

APPENDIX B MORE EXAMPLES OF QUERY GRAPH

Fig. 13 presents more examples of our redefined query graphs.

APPENDIX C SUPERVISED SIGNAL BUILDING FOR HGNET

The supervised signals for training HGNet, i.e., \mathcal{A}_o , \mathcal{A}_v , and \mathcal{A}_e , are obtained in Algorithm 2.

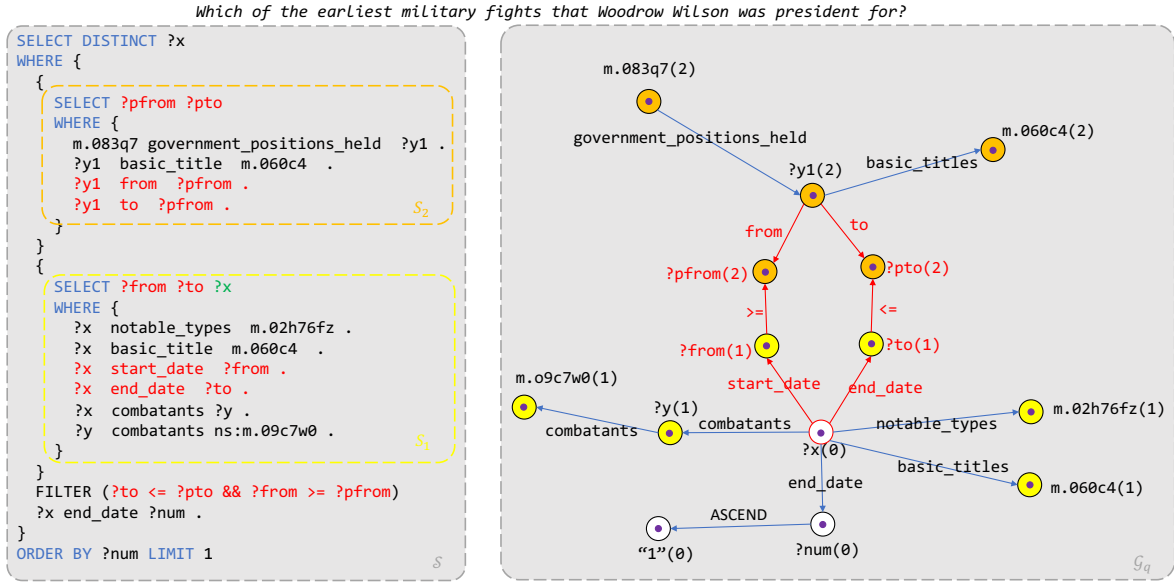
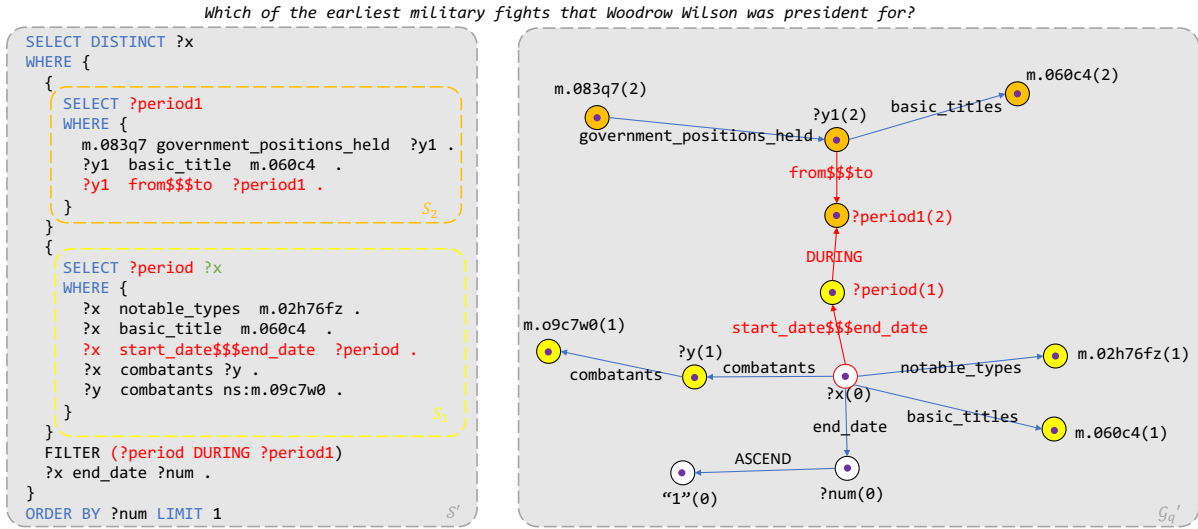
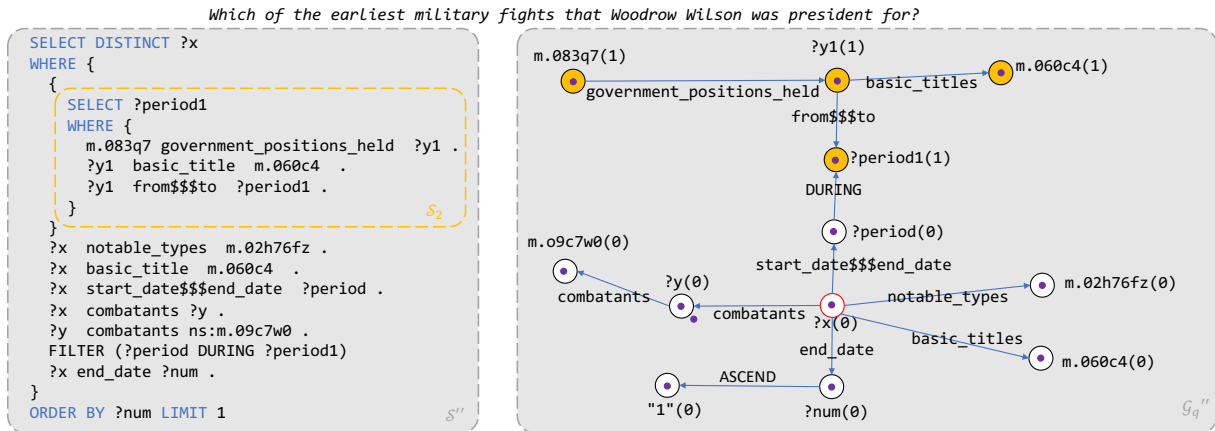
The total process is regarded as a traversal on gold query graph \mathcal{G}_q^+ . The traversal is started from vertex v_{Ans} , which is the vertex of class Ans because each query graph must have a vertex denoting the answer.

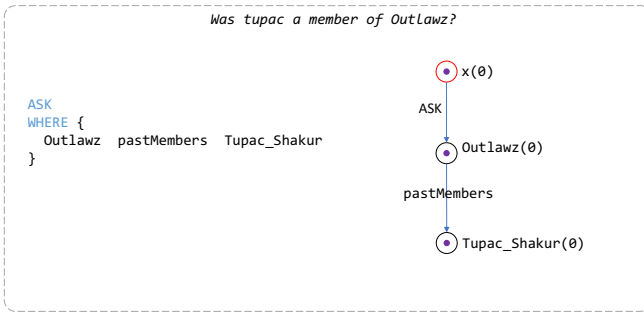
At the beginning of traversal, $[Ans, 0, NONE]$, the arguments of the first operation *AddVertex*, are pushed into \mathcal{A}_o (line 26 in Algorithm 2) and NONE, the instance of v_{Ans} is pushed into \mathcal{A}_v (line 27 in Algorithm 2).

Thereafter, each vertex of \mathcal{G}_q^+ will be visited by the depth-first traversal. Supposed that u is the vertex currently being visited and its neighbor vertex v along an outgoing edge $e^+ = \langle u, v \rangle$ is the next vertex to be visited. If regarding the step from u to v as an expansion process that adding v to connect to u , the step includes three *Outlining* operations, namely *AddVertex*, *SelectVertex*, and *AddEdge*. Three groups of arguments are $[c_v, s_\delta, \hat{v}]$, $[u]$, and $[c_{e^+}, \hat{e}^+]$, respectively (line 10-12). Here, c_v and c_{e^+} are the class labels, s_v denotes the segment number of v , and \hat{v} and \hat{e}^+ denotes the vertex

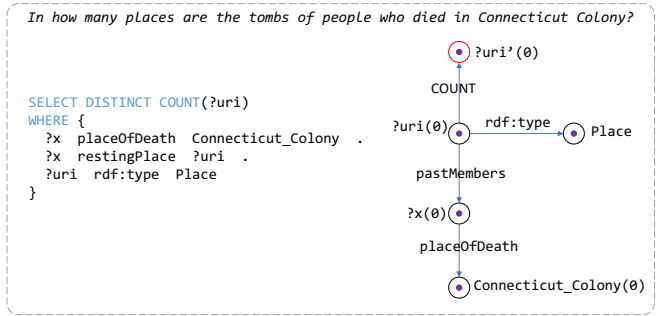
and edge to be copied by v and e^+ , respectively. If there is no vertex (edge) to copy, $\hat{v} = NONE$ ($\hat{e}^+ = NONE$). In addition, the two *Filling* operations, *FillVertex* and *FillEdge* can be obtained according to the *AddVertex* and *AddEdge*. Two arguments are i_v , and i_{e^+} , respectively (line 13-14). For the traversal step along the incoming edge $e^- = \langle v, u \rangle$, the process is similar (line 17-21). After the arguments of this step are obtained, the traversal continues from v .

Once all vertices are visited, the traversal is completed. Finally, a group of arguments $[End, 0, NONE]$ is pushed into \mathcal{A}_o and it denotes the signal of ending. *Outlining*.

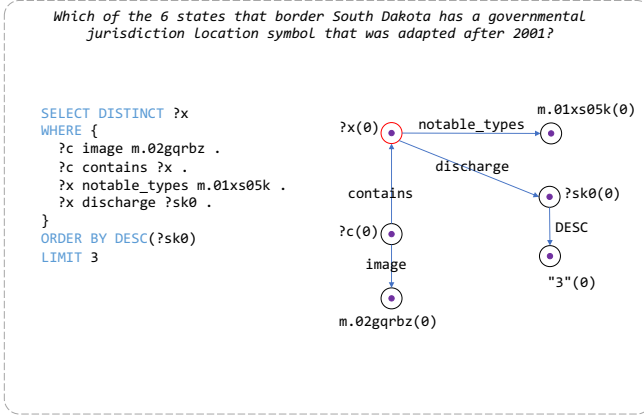
Fig. 10: An example SPARQL program \mathcal{S} having the constraint of temporal interval and the sub-query with $?x$ intention.Fig. 11: \mathcal{S}' and \mathcal{G}_q' obtained by removing the cycle path of temporal intervals.Fig. 12: \mathcal{S}'' and \mathcal{G}_q'' obtained by simplifying $?x$ intention, which are used for training HGNet.



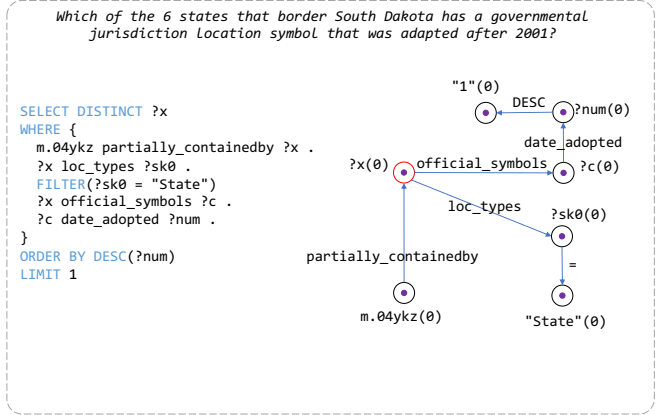
(a)



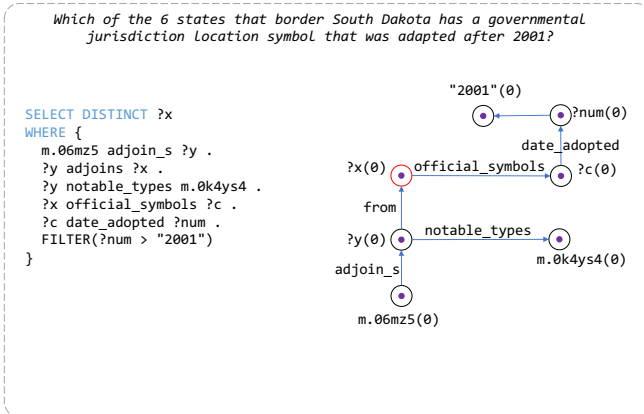
(b)



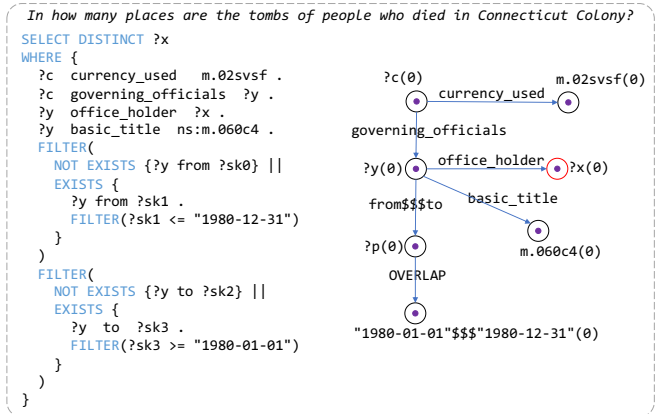
(c)



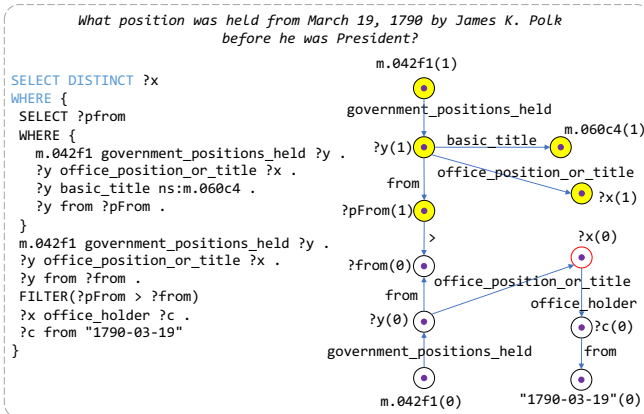
(d)



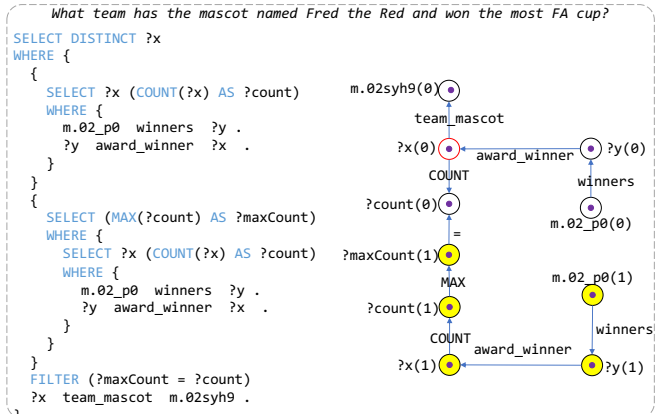
(e)



(f)



(g)



(h)

Fig. 13: More examples of our redefined query graphs. Red denotes the answer vertex.